KERNFORSCHUNGSANLAGE JÜLICH
GESELLSCHAFT MIT BESCHRÄNKTER HAFTUNG
Institut für Festkörperforschung

Metallographic Investigations of Group Vb Metal-Hydrides

Part I: β-Phase Melting and Solidification Phenomena in the Niobium-Hydrogen System

Part II: Techniques for the Metallographic Examination of Niobium-, Tantalum- and Vanadium-Hydrides

by

T. Schober, U. Linke and H. Wenzl

Jül - 1240
Oktober 1975

Als Manuskript gedruckt

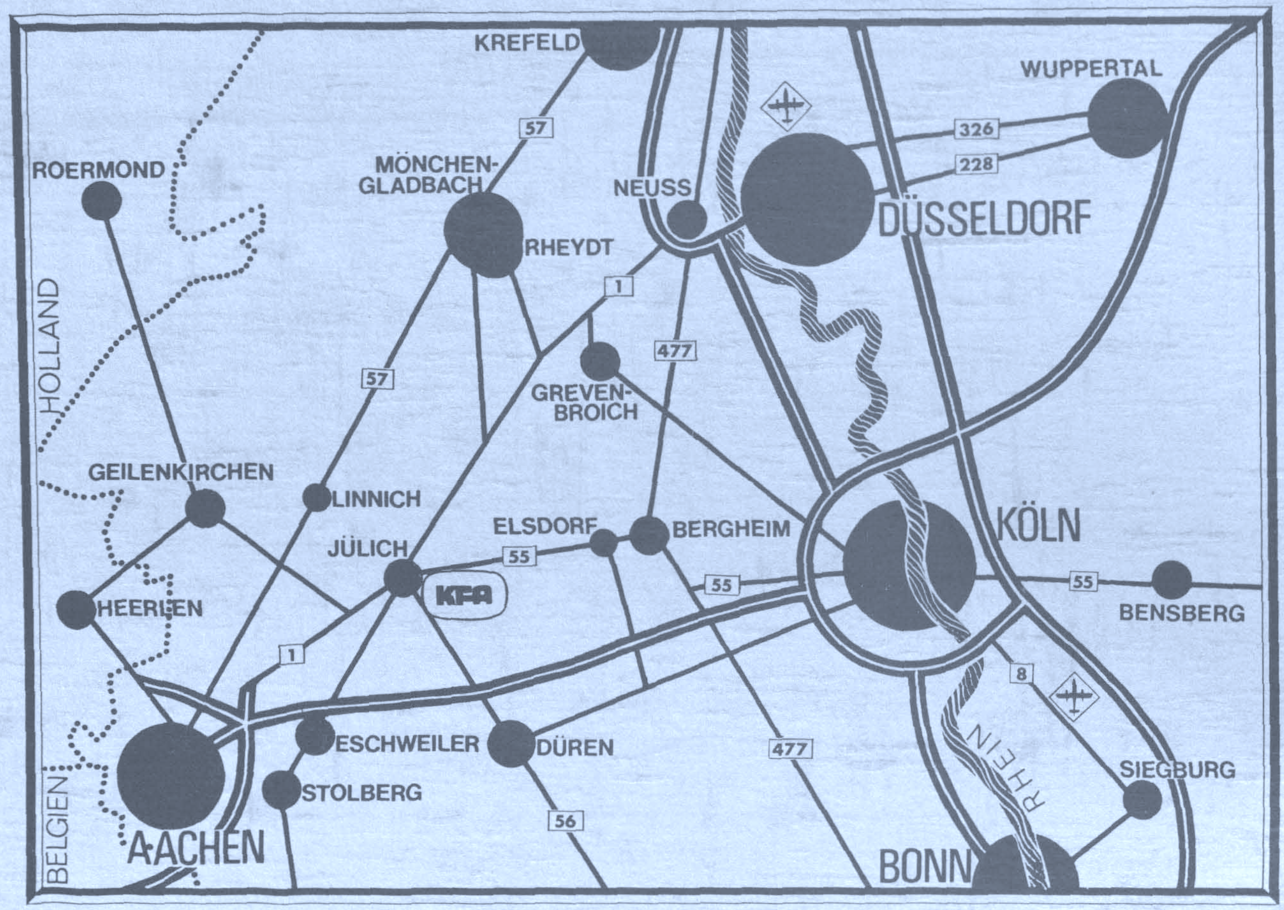

Berichte der Kernforschungsanlage Jülich – Nr. 1240

Institut für Festkörperforschung Jül - 1240

Dok.: Metal-Gas System - Nb-H, Morphologies
Nb-H System - Optical Metallography
Nb-H System - β-Phase, Melting, Solidification
Nb-H System - Morphologies
Nb-H System - Phase Transformation
NbH - Optical Metallography
TaH - Optical Metallography
VH - Optical Metallography

Im Tausch zu beziehen durch: ZENTRALBIBLIOTHEK der Kernforschungsanlage Jülich GmbH, Jülich, Bundesrepublik Deutschland

Metallographic Investigations of Group Vb Metal-Hydrides

Part I: β-Phase Melting and Solidification Phenomena in the Niobium-Hydrogen System

Part II: Techniques for the Metallographic Examination of Niobium-, Tantalum- and Vanadium-Hydrides

by

T. Schober, U. Linke and H. Wenzl

Abstract (Part I)

The morphology of the decomposition and formation (or the melting and solidification in the lattice gas description) of the ordered NbH β-phase is investigated with polarized light and interference contrast techniques. Melting occurs in the absence of temperature gradients by the growth of droplets of the liquid phase α' nucleated at the domain boundaries. Solidification of the α'-phase involves the formation of single-domain β-phase plates, subsequent repeated twinning and the growth of "elastic closure domains". The solidus and liquidus lines of the $\beta \rightarrow \alpha'$ transformation are determined in the range from 70 to 95 at. % H/Nb where the transition temperatures vary from $84^{o}C$ (triple line of α-, α'- and β-phase) to $145^{o}C$.

1. Introduction

The NbH system has been extensively studied in the last years, both experimentally and theoretically. Only quite recently has detailed information been obtained on the morphological aspects of the precipitation of some of the hydrides, see for example, (1-5). In the NbH phase diagram in Fig. 1 and in the figure caption the known hydride phases are presented. Of prime importance here are the ordered hydride phases β, ζ and ε among which only the β-phase is stable at or above room temperature. Fig. 2 shows the structure of the β-phase. It has an orthorhombic unit cell which may conveniently be described by the vectors $\vec{a}$, $\vec{b}$ and $\vec{c}$. (Details in figure caption.) It is the purpose of the present work to present polarized light and interference contrast observations on the morphology of the $\beta \rightarrow (\alpha + \alpha')$ or $\beta \rightarrow (\beta + \alpha') \rightarrow \alpha'$ phase transformations. Also, transformations occurring in the reverse direction were studied. In the lattice gas terminology (Alefeld (6)) used in this work we consider the ordered β-phase the solid which may melt at the transition temperature to give the disordered liquid phase α'. Also, sublimation of β may occur, resulting in the gaseous phase α. At concentrations above 70 %, solid β may only transform to the liquid α'. In this nomenclature the present work deals with melting and solidification effects of the solid β-phase. It is noted that the NbH system is exceptional in the sense that the formation and the decomposition of the ordered β-phase occurs rapidly at relatively low temperatures (of the order of $100^{o}C$) and may directly be observed on the surface of well polished single crystal specimens. During the α'-β transformation the hydrogen atoms need only jump to adjacent interstitial sites. The high speed of the transformation and the low transition temperature are due to the high jump rates (10^{10} sec^{-1}) and low binding energies of the hydrogen atoms to the precipitates.

2. Experimental

Details of the experimental procedure may be found elsewhere (2, 3, 7). In brief, single crystal sections of Nb were charged electrolytically with hydrogen to the indicated concentrations. The resulting hydride specimens were then embedded in resin, ground and polished as outlined in detail in (7). Visual inspection with polarized light after the final polish revealed whether the damaged surface layer had been removed. In this case the domain structure of the β-phase could be observed. The samples were then clamped onto a special heating stage (7) and observed with polarized light with nearly crossed polarizer and analyzer, and at constant or slowly increasing or decreasing temperatures. The domain structure was sequentially photographed on 24 x 36 mm film or filmed with a 16 mm movie camera. Normarski interference contrast was also found useful to study the $\alpha' \rightarrow \beta$ transformation since it revealed the surface tilts which occurred locally when an area transformed to the anisotropic β-phase. (For this point see (3).)

3. Results

3.1 Melting of the β-phase

The onset of β-phase melting may generally be recognized in polarized light by the appearance of the optically isotropic phases α or α' which have a uniform grey shade as opposed to the domains of β which appear either bright or dark.

In the concentration range from 5 to 70 % the appearance and complete formation of the transformation products α and α' took place within $1^{o}C$ starting at $84^{o}C$. The morphological features of the phase transition were the same as described below for higher concentrations where the transition is extended over several degrees C. Fig. 3 shows a series of photographs of the melting of an 80 % NbH alloy. It is seen that α' appeared in the form of small facetted prisms bounded by {100}, {110} or {211} planes. It could be clearly seen that nucleation of α' occurred along the domain boundaries of the β-phase. The α'-prisms increased in size with increasing temperature until only a few multiply twinned β-particles remained which often had a geometry similar to the one shown in Fig. 4a. Here, four domains (β-1 to β-4) are drawn. The boundary between β-1 and β-2 is a fully coherent twin boundary whereas the other boundaries are incoherent. Domains β-3 and β-4 may be referred to as "elastic closure domains" which reduce the strain energy at the ends of domains β-1 and β-2. They are analoguous to the well-known magnetic closure domains. Fig. 4b shows an actual example of a particle as described in Fig. 4a.

The above features of local melting at the domain boundaries were generally observed when no apparent gradient of temperature existed along the specimen surface.

When temperature gradients existed on the surface a melting front advanced through the sample. A typical sequence is shown in Fig. 5 where the solid-liquid interface moved from the right to the left hand side. Fig. 5 also clearly demonstrates that a considerable motion and rearrangement of domain boundaries occurred just prior to melting. This domain boundary migration was most probably caused by stresses due to temperature gradients.

It can be easily visualized how domain boundaries could migrate by the movement of steps on their surface as shown in Fig. 6a and b. All that is required to move the step in Fig. 6a is the motion of a chain of hydrogen atoms along [001] from z = 1/4 to z = 3/4 positions (see arrows in Fig. 6a, b). The chain itself may be moved by the migration of a kink along the step.

3.2 Solidificaiton of the β-phase

Fig. 7 shows the formation of β-phase particles and subsequent growth when a hydride is slowly cooled from the liquid α'-phase into the (α' + β) region. The individual steps in this process are schematically outlined in Fig. 8a, b, c,. First, the appearance of single-domain plates is observed (Fig. 7a and 8a). The model in Fig. 8a shows that the vicinity of the initially coherent β-plates is elastically distorted in such a way that hydrogen is attracted to the tips and the sides of the plate. Furthermore, it is seen that the elastic distortions are partially alleviated if new domain plates of opposite distortions are nucleated at the sides (Fig. 8b). The boundaries betwen the domains would be coherent twin boundaries. Further growth involves the elongation of the initial plates, repeated twinning and the formation of closure domains at the tips of the growing domain plates (Fig. 8c).

A comparison of the transition temperatures upon heating or cooling revealed that supercooling of α' was possible to the extent of several degrees C. For this reason the transition temperatures were always measured upon heating of the samples.

3.3 The β-α' phase boundaries

Since the temperature of the first appearance of α'-nuclei and the complete disappearance of β could be measured for a given NbH alloy, it was possible to determine the β-α' phase boundaries using a number of samples with concentrations between 70 and 95 %. The result is shown in Fig. 9. The considerable scatter of the data is believed to be due to inhomogeneities in the hydrogen concentrations and the uncertainities in the temperature and hydrogen concentration measurements. It is however clear that the temperature range of the β-α' two phase region is very narrow (of the order of a few degrees ^{o}C) around 75 to 80 at. % H/Nb. It becomes wider at higher concentrations and reaches 10-12^{o}C at 90 to 95 at. %.

4. Discussion

The present results demonstrate that melting of the β-phase occurs at well defined temperatures which give the β-α' solidus at concentrations above 70 %. No evidence for any "premelting effects" (8) was found in the course of the study. The nucleation of droplets of the α'-melt at the domain boundaries (Fig. 3) is not surprising since elastic distortions and disorder exist at these interfaces which lower the free energy of possible α'-nuclei. Analogous observations were made for the case of grain boundaries (Glicksman and Vold (9)) and discussed in that work in great detail.

The solidification of α' apparently occurred in such a way as to minimize the distortions of the host lattice. This may only be accomplished by the nucleation of thin plates of β and subsequent repeated twinning. - The high-concentration region of the phase diagram determined with the present technique is qualitatively in agreement with the classical Walter-Chandler work (10) and with further measurements (11).

Acknowledgement

Valuable technical assistance was provided by U. Linke, A. Brusch-Meisenberg and C. Mambor.

References

1) M.S. Rashid and T.E. Scott, J. Less-Common Metals 31, 377 (1973)
2) T. Schober, U. Linke and H. Wenzl, Scripta Met. 8, 805 (1974)
3) T. Schober and U. Linke, J. Less-Common Metals, in print (1975); also available as JÜL-Report Nr. 1192
4) T. Schober, phys. stat. sol. (a) 29, 395 (1975); 30, 107 (1975)
5) T. Schober, M.A. Pick and H. Wenzl, phys. stat. sol. (a) 18, 175 (1973)
6) G. Alefeld, phys. stat. sol. 32, 67 (1969)
7) T. Schober and U. Linke, Metallography (in print)
8) M.A. Pick, B. Alefeld, J.-M. Welter, to be published
9) M.E. Glicksman and C.L. Vold, Surface Science 31, 50 (1972)
10) R.J. Walter and W.T. Chandler, Trans. Met. Soc. AIME 233, 762 (1965)
11) J.-M. Welter (to be published)

Figure Captions

Fig. 1: Phase diagram of the NbH-system: α and α' are disordered b.c.c. solutions, β, ε and ζ are ordered orthorhombic phases. δ is a f.c.c. phase of composition NbH_2 and γ a low-temperature b.c.c. phase.

Fig. 2: Structural model of the NbH β-phase. The hydrogen atoms occupy tetrahedral positions aligned along [110]. Assuming a repulsive interaction between hydrogen atoms in these chains an elongation of the unit cell along b would occur with $b > a \simeq c \cdot \sqrt{2}$.

Fig. 3: a) to h) Series of polarized light micrographs of the "melting" of a 80 % β-NbH alloy in the absence of temperature gradients. The black dot is located in identical positions on all pictures.

a) Room temperature appearance; two alternating domains of β-NbH are visible, b) T = 112°C, small prisms of α' appear along domain boundaries. c-e) 113°C, growth of α'-prisms, f-h) 114°C, α'-regions grow continuously and leave behind a few multiply twinned particles (h) which are also rapidly dissolved.

Fig. 4: a) Schematic drawing of a twinned particle which frequently occurred upon melting or solidification. The subscript p denotes a projected direction.

b) Example of a particle as outlined in a).

Fig. 5: a) to f) Series of polarized light micrographs of the "melting" of a 93 % β-NbH alloy in the presence of a temperature gradient. The black dot is located in identical positions on all pictures.

a) Room temperature appearance of domains,

b) T = 150°C, melting front appears in upper left hand corner.

Arrows denote where a movement of domain boundaries has occurred in a) and b) (and c)).

c-e) Melting front advances to right hand corner.

f) A few single domain plates or twinned plates of β still remain in liquid α' and will soon disappear.

Fig. 6: a) and b) Movement of steps upon applying shear stress τ on coherent domain boundary. The steps advance when hy-

drogen atoms are moved from $z = \frac{1}{4}$ to $z = \frac{3}{4}$ positions - see arrows. Nb atoms are omitted (see Fig. 2).

Fig. 7: a) to f) Series of micrographs in interference contrast showing solidification of liquid phase α'.

a) Appearance of single domain plates of β upon cooling to 115°C.

b) Stress relief is accomplished by twinning of single domain plates.

c-e) Growth and coalescence of multiply twinned particles.

f) Final state after solidification.

Fig. 8: Schematic illustration of β-phase formation (solidification of α'). Shaded areas are β-phase regions - one shade of grey corresponds to each of the domain orientations.

a) A single domain plate of β is nucleated. $\vec{a}$, $\vec{b}$ and $\vec{c}$ are unit vectors of the orthorhombic structure.

b) Further domain plates of opposite distortions grow at faces of the original plate. The distortions around the first plate are minimized by the formation of coherent domain boundaries.

c) Further growth and formation of "closure domains".

Fig. 9: The β-α' phase boundaries. Filled circles are experimentally determined transition temperatures. The upper temperature of a pair of measurements corresponds to the complete disappearance of β upon heating; the lower to the first appearance of α'; the uncertainties in the concentrations are approximately $\pm$ 5 at. % H/Nb.

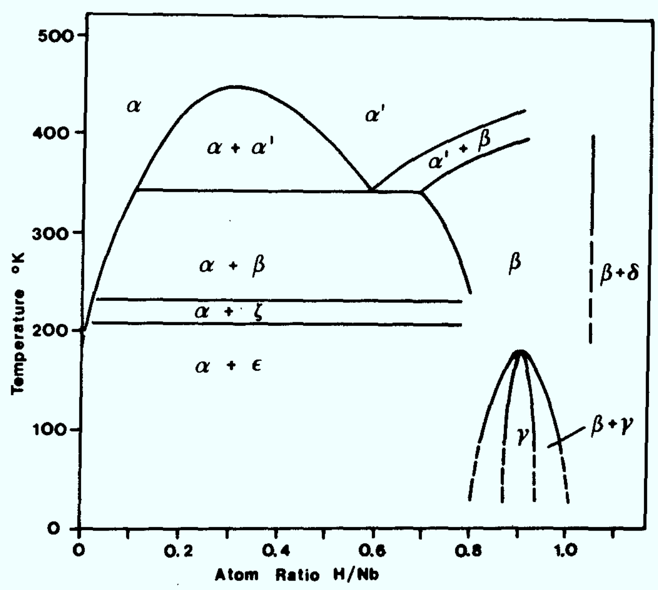

500
400
300
200
100
0
Temperature °K
α
α + α'
α'
α' + β
α + β
β
β+δ
α + ζ
α + ε
γ
β+γ
0
0.2
0.4
0.6
0.8
1.0
Atom Ratio H/Nb

Fig. 1 (I)

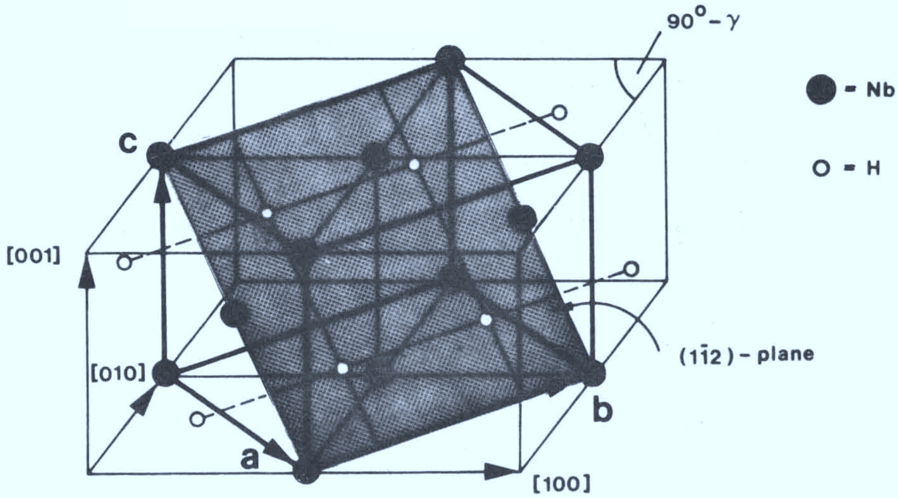

Fig. 2 (I)

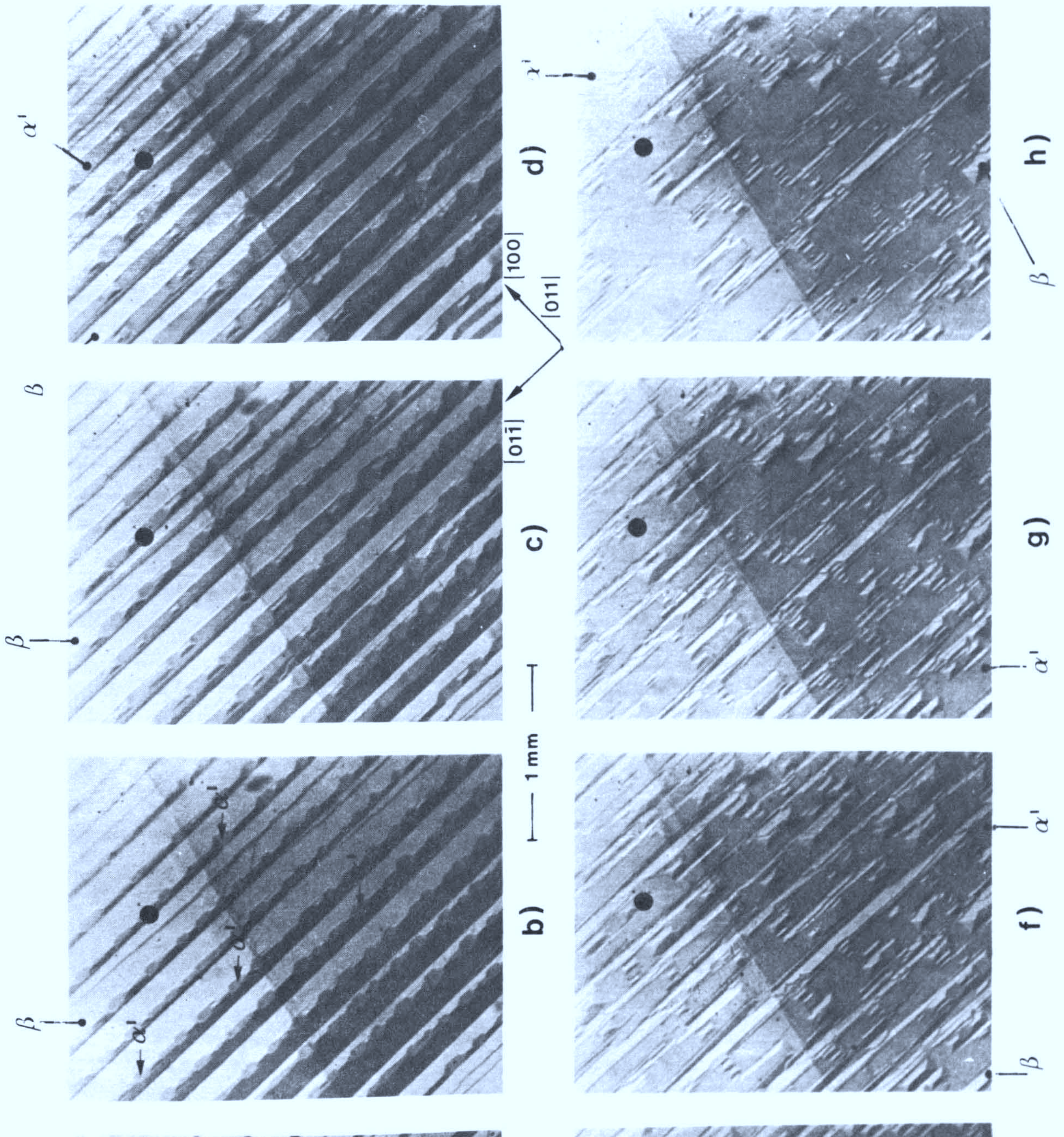

Fig.3a-h (I)

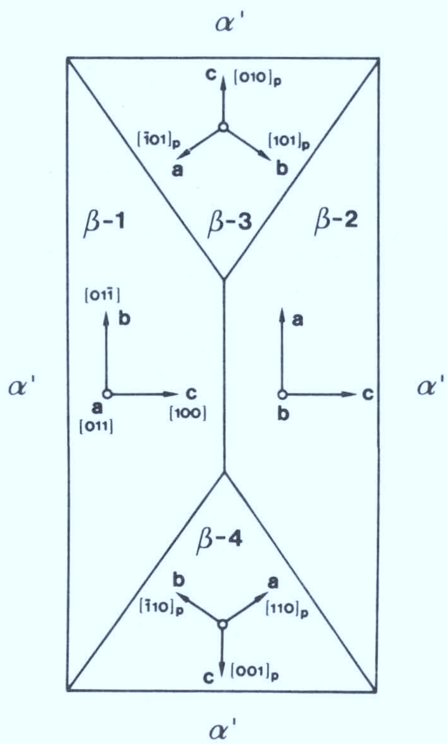
α'
c [010]p
[1̄01]p
[101]p
a
b
β-1
β-3
β-2
[011̄]
b
a
a
c
[011]
[100]
b
c
α'
α'
β-4
b
a
[1̄10]p
[110]p
c [001]p
α'

a)

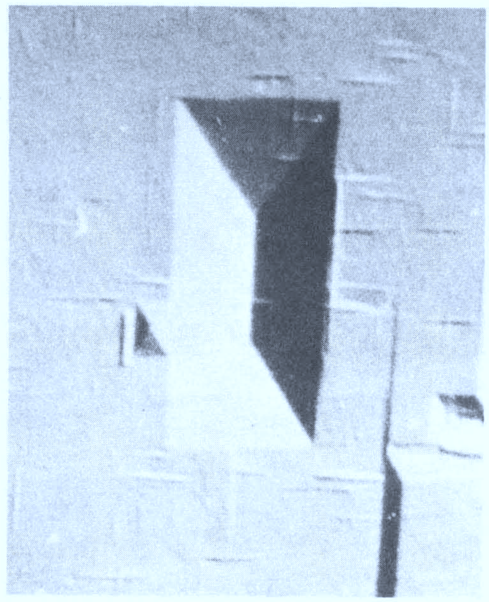

b)

Fig. 4a,b (I)

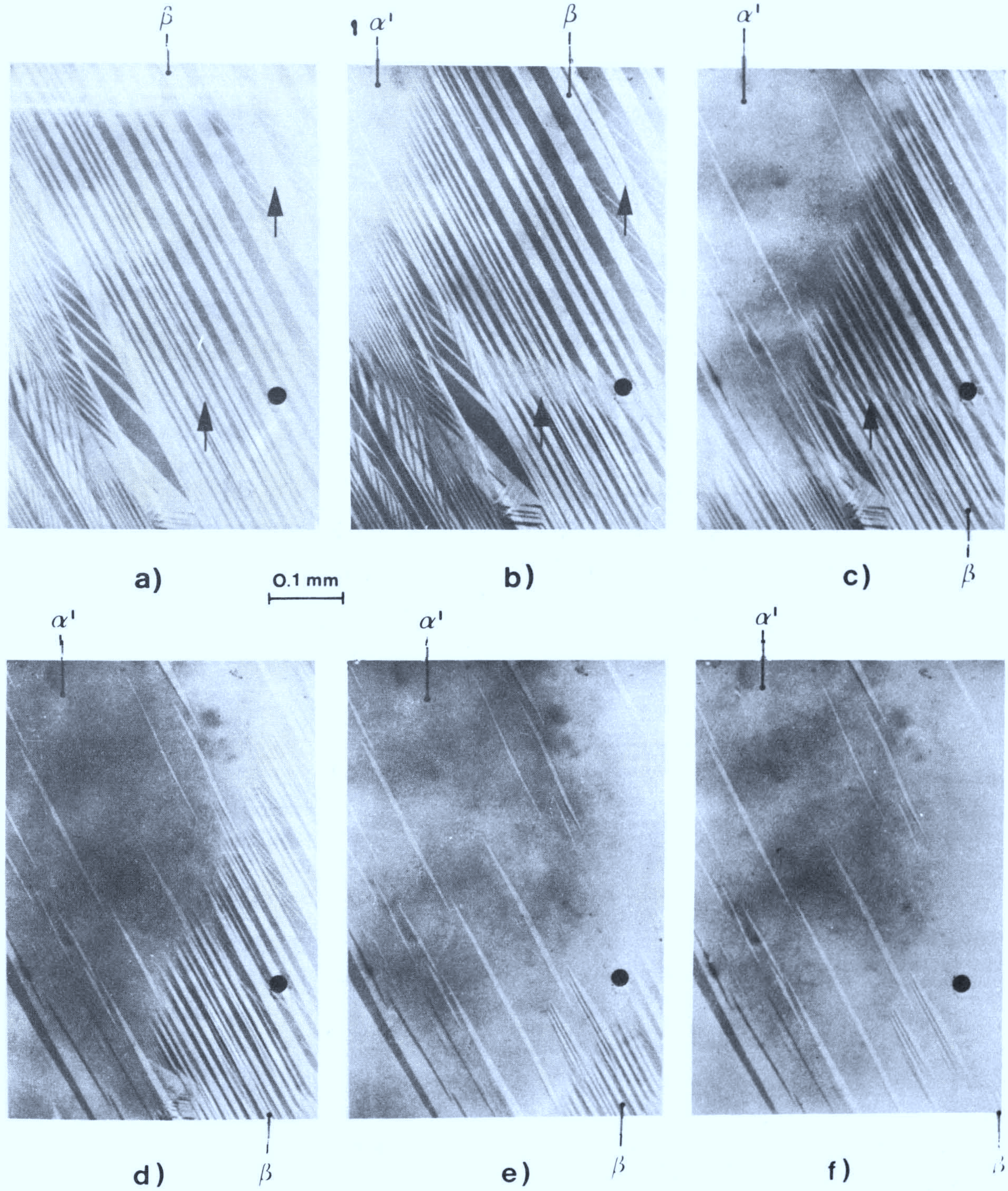

Fig. 5a-f (I)

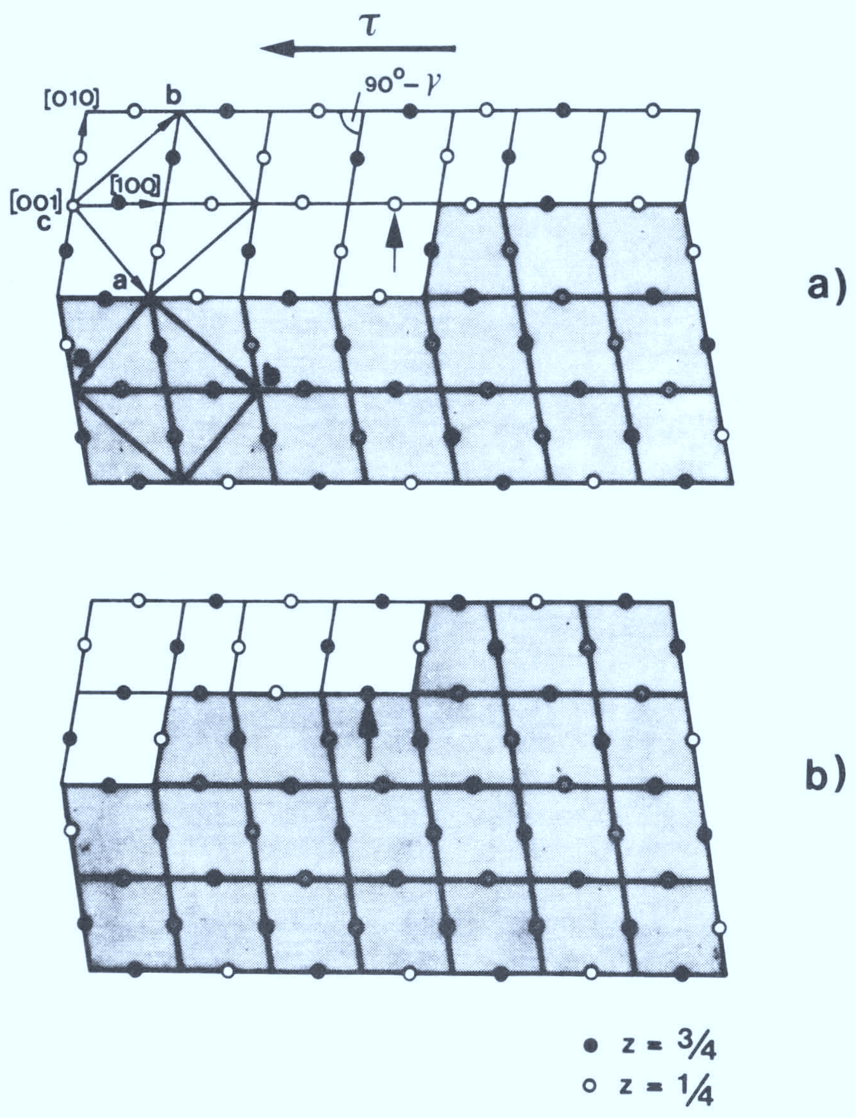

Fig. 6a,b (I)

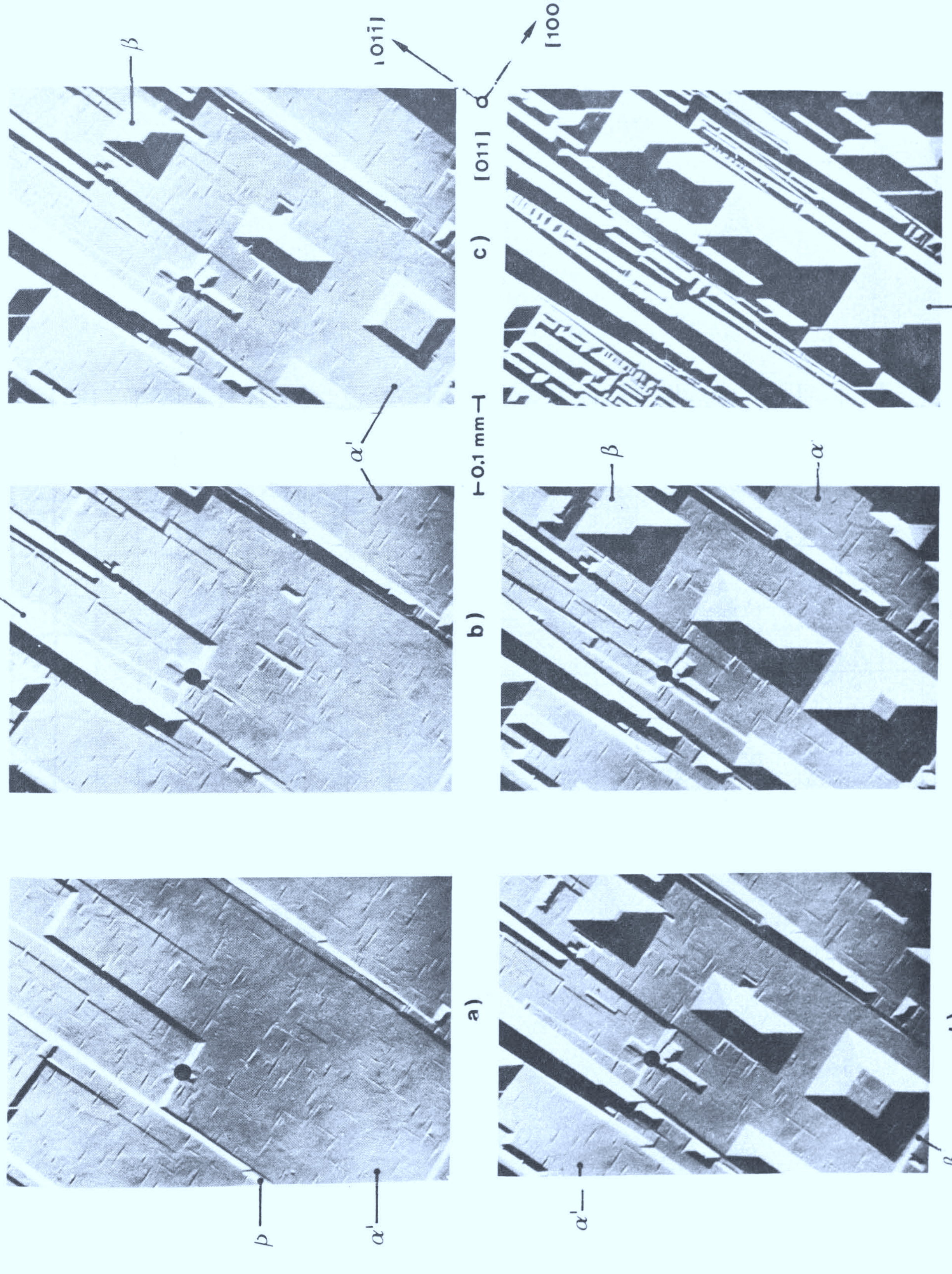

Fig. 7a-f (I)

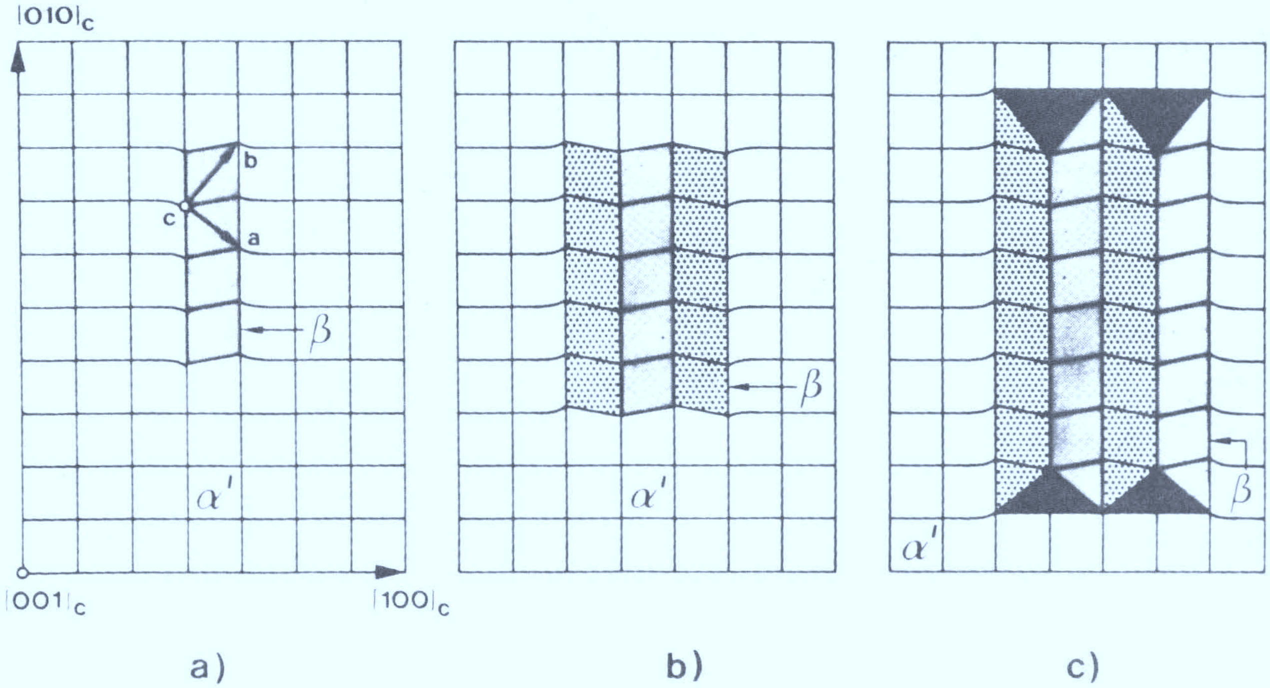

Fig.8a,b,c (I)

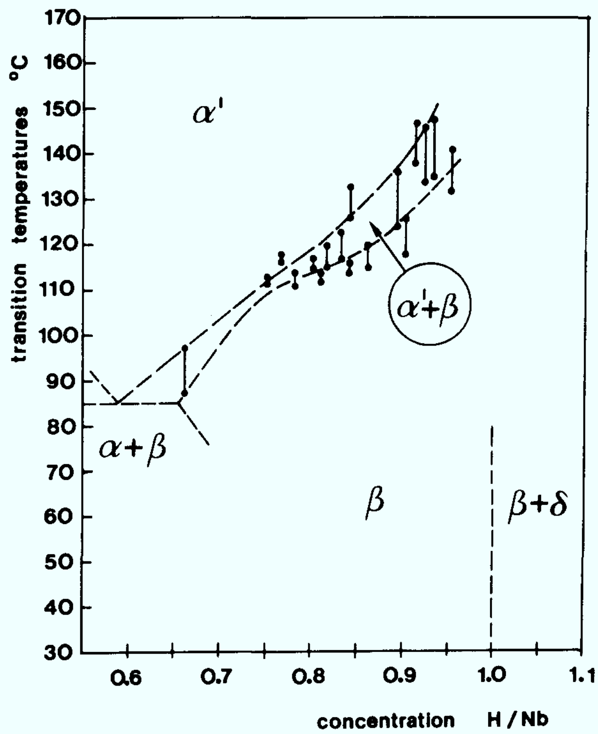

170
160
150
140
130
120
110
100
90
80
70
60
50
40
30
transition temperatures °C
α'
α'+β
α+β
β
β+δ
0.6
0.7
0.8
0.9
1.0
1.1
concentration H / Nb

Fig.9 (I)

Abstract (Part II)

Techniques for the metallographic examination of Nb, Ta and V-hydride specimens are presented. Special sample mounting procedures, as well as a heating and a cooling stage suitable for hydride investigations are described. The application of polarized light observations and Nomarski interference contrast to the study of hydrides is discussed. Some examples of micrographs of Nb, Ta or V-hydrides are given.

Introduction

The metal-hydrogen systems have received considerable attention during the last years. This was due to their technological as well as scientific importance. Of particular interest were the exothermic occluders of hydrogen, among which the group Vb metals Nb, Ta and V played a dominant rôle. The hydrides of the latter metals were the subject of several previous metallographic studies (1-8) and of extensive recent investigations by the present authors (9, 10). In the course of the latter work, a number of techniques for the metallographic examination of Nb, Ta and V-hydrides were developed which will be reported in this paper.

Specimen Preparation

The Nb, Ta, V-hydrides (MeH) specimens were produced either by gas phase charging in a UHV system or by electrolytic charging in orthophosphoric acid at roughly 150°C (9, 10). By varying the charging time for the latter process a large number of different MeH alloys were obtained. The starting material was high purity single crystals of known orientations which had been UHV-degassed (with the exception of V).

The resulting MeH-samples were often rather brittle and contained cracks. For the room temperature observations the samples were embedded in castable polyester resin[1)] using standard techniques. Alumina fillers were used to improve on the polishing characteristics of the resin. For the cooling and heating stage observations, the MeH-samples were first embedded in a 8 mm diameter SS 304 ring using a one-component silver epoxide[2)]. Subsequently, this ring was mounted in castable polyester resin (see Fig. 1). After polishing was completed the ring was freed from the surrounding resin with a saw[3)] and clamped onto the heating or cooling stage. In this way a composite sample was obtained which had parallel sides and could be heated to 200°C in air or cooled to -196°C in vacuum. In cases where no temperatures above 140°C were required, the silver epoxide could be replaced by the above castable resin filled with copper powder.

---

1) Scandiplast (Tempelmann)

2) Bostik 2970-Elecolit 312 (Bostik GmbH)

3) If properly done, this operation did not induce any deformation or scratches on the polished surfaces.

Grinding was succesively done with 320, 400 and 600 mesh SiC paper, followed by diamond polishing (15-6-3 µm grain size for 30 min). The latter polish was discontinued when no visible SiC particles could be detected anymore on the surfaces. Finally, vibratory polishing was carried out for 2-3 days using a 0.3 µm Al_2O_3 ferrocyanide slurry (1 part saturated solution to 5 parts H_2O). This last step was found to be very important for the polarized light observations of the domain structures of the MeH-alloys. Attempts to produce well polished surfaces by electrolytic polishing were unsuccessful.

Methods of Examination

The microscopic observations of the polished MeH alloys were carried out on an Reichert inverted stage MeF2 microscope in bright and dark field, with polarized light at almost crossed polarizers, or using Nomarski interference contrast. The temperature during observation could be varied from $-196^{o}C$ to roughly $+200^{o}C$ with the use of the cooling and heating stages described below.

Bright field observations were helpful in identifying the hydride phases in the b.c.c. matrix after etching. As an example, Fig. 2 shows thin plates of the V-H β-phase embedded in the α-phase (details in Figure Caption). Similarly, precipitation of dihydride phases (MeH_2) in the monohydride (MeH) could readily be observed on the etched samples. This is illustrated in Fig. 3a for the case of NbH_2-precipitation in the β-phase (NbH). The identical area is shown in Fig. 3b in polarized light (see also below). The use of single crystal specimens allows here for the unambiguous determination of precipitate habit planes. The dendritic hydride precipitation which arise at high supersaturations and high cooling rates (9, 10) may already be observed in bright field on the surface of unpolished MeH samples as shown in Fig. 4

Dark field techniques were used to image small quantities of a new phase inside the parent phase. As an example we present NbH_2 precipitation inside the NbH matrix (Fig. 5).

Polarized light observations were extremely useful in identifying non-cubic, anisotropic phases and in revealing their domain structure. Ordering of hydrogen in the Me-b.c.c. lattice leads to anisotropically distorted phases with orthorhombic (Nb, Ta, (11)) and monoclinic structure (V (12)). Under the usual conditions of almost crossed polarizer and analyzer the domain structures could be made visible. The following points, however, were of importance:

- The surface of the specimens had to be virtually free of deformation layers (for this reason long vibratory polishing was essential).
- A given domain or pair of domains may be "out of contrast" for a specific angle of rotation of the specimen stage. Therefore, the same area should be examined at different angles of rotation and at different settings of the analyzer to ensure that the complete domain structure is imaged.
- Crystallographic information on the domains (i.e. habit planes) may be obtained by photographing different (hkl)-planes of the Me-H "single"-crystal.

As an example for domain structures we present in Fig. 6 a polarized light micrograph of a β-TaH alloy. It is seen that the domain boundaries are crystallographically oriented and predominantly situated on low index planes of the matrix. The domain images often had a 3-dimensional appearance which in Fig. 6 stemmed from the 3 shades of grey in the picture. Finally, polarized observations permitted one to reveal precipitation of the cubic phases of type MeH_2 inside the optically anisotropic β-phases of type MeH as shown in Fig. 3b for NbH_2 precipitates.

Nomarski interference contrast observations were found useful in studying

- two-phase regions were the two phases differ in hardness and where a surface relief is present,
- deformations of the surface arising from phase transformations occurring in the samples after polishing.

Examples of the first point may be found in Rf. (10). The second point is illustrated for the case of transformations occurring in the ordered compound of type MeH. In Fig. 7a a model of the domain structure of β-NbH is shown. The top surface has received a good polish and is flat. The orthorhombic structure is then allowed to transform to the cubic phases γ or α. The previously flat surface contains now slightly inclined sections (Fig. 7b) outlining the shape of the original NbH-domains. An illustration of the above effect is presented in Fig. 8a,b for the case of the $\beta \rightarrow \gamma$ transformation in the Nb-H system (details in Figure Caption).

Plastic deformation also gave rise to a surface relief which corresponds to the original domain configuration. Since plastic deformation effects accompanied the above phase changes, multiple transitions through the phase boundary generated a superposition of two or more different domain patterns on the surface. This "memory effect" for the domain configurations previously present on the surface is shown in Fig. 9 for a NbH alloy which had been heated twice above the $\alpha' \rightarrow (\alpha' + \beta)$ phase boundary.

The heating stage (see Fig. 10) was mainly used to study the decomposition of the ordered alloys of type MeH at elevated temperatures. It also served to determine the exact transition temperatures. A typical polarized light sequence of the order disorder reaction occurring in a NbH alloy is shown in Fig. 11a, b, c. Some of the transitions were filmed with a 16 mm motion picture camera.

The cooling stage in Fig. 12 was instrumental in observing the low-temperature transitions such as the $\beta \rightarrow \gamma$ transition in the NbH system shown in Fig. 8a, b. It was also used to determine the low-concentration phase boundaries of the MeH systems since the precipitation of hydrides may readily be observed on the surfaces of well polished samples. Here, features rather similar to the dendritic hydrides in Fig. 4 may be observed.

Concluding Remarks

The present techniques should enable the interested reader to examine successfully various group Vb metal hydrides. Together with the results of our previous study on Nb (10), an assessment of concentrations and phase distributions in these metal hydrides should be rather straightforward.

References

1) Y. Sasaki and M. Amano, Trans. Japan Inst. Metals 8, 276 (1976).
2) M. Amano and Y. Sasaki, phys. stat. sol. (a) 19, 405 (1973).
3) M.S. Rashid and T.E. Scott, J. Less-Common Metals 31, 377 (1973).
4) G.C. Rauch, R.M. Rose and J. Wulff, J. Less-Common Metals 8, 99 (1965).
5) D. Hardie and P. McIntyre, Metal Sc. J. 6, 40 (1972).
6) J. Wanagel, S.L. Sass and B.W. Batterman, Met. Trans. 5, 105 (1974).
7) D.G. Westlake, J. Less-Common Metals 23, 89 (1971).
8) D.H. Sherman, C.V. Owen and T.E. Scott, Trans. TMS-AIME 242, 1775 (1968).
9) T. Schober, U. Linke and H. Wenzl, Scripta Met. 8, 805 (1974).
10) T. Schober and U. Linke, JÜL-Report Nr. 1192
11) M.A. Pick, International Meeting on Hydrogen in Metals, Jülich (1972).
12) J. Wanagel, S.L. Sass and B. Batterman, phys. stat. sol. (a) 11, 767 (1972).

Figure Captions

Fig. 1: Illustration of Me-hydride sample mounting for the heating and cooling stages. (The SS 304 ring together with the sample is clamped onto the stages.)

Fig. 2: Thin plates of β-VH in α-phase. $c_H \simeq 12$ %. Habit plane is (10 3 3) (6). The sample was slightly etched.

Fig. 3: Nb-dihydride (δ-phase) precipitation inside the monohydride (β-phase). $c_H \simeq 130$ %.

a) Plates of the δ-phase inside the β-phase after etching. Habit plane is (210) (9, 10). Bright field.

b) The same area but photographed with polarized light before etching. The domain structure of the β-phase is partially visible. Note that δ-phase plates are optically isotropic as is expected from a cubic phase.

Fig. 4: Dendritic NbH β-phase precipitates as directly seen on a surface which had been chemically polished prior to hydrogenation.

Fig. 5: Dark field image of NbH_2-precipitates (δ-phase) inside the β-phase. Sample was slightly etched. Precipitates are not yet visible in polarized light in the unetched condition.

Fig. 6: Domain structure of a β-TaH alloy. One shade of grey corresponds to one domain of the β-phase. Polarized light photograph. The 3-dimensional appearance of the polished sample arises from the 3 different shades of grey.

Fig. 7: Illustration of surface tilts arising from phase transformations after polishing (after (10)).

a) Schematic drawing of a 3-domain β-NbH crystal. Arrows denote domain boundaries. The orthorhombic unit cells with basis vector $\vec{a}$, $\vec{b}$ and $\vec{c}$ are shaded. A possible (110) cleavage plane is shown, it consists of slightly tilted sections. Top surface is polished and flat.

b) Sample is allowed to transform to the cubic structure ($T > 85^{\circ}C$). The surface contains now tilted sections outlining the domain geometry in a). These tilts may readily be seen with interference contrast.

Fig. 8: Surface tilts arising from the orthorhombic to cubic ($\beta \to \gamma$) transformation in the NbH-system. $c_H \approx 87$ %.

a) Room temperature micrograph of a β-phase area after polishing. Interference contrast. Some surface relief due to domains is visible.

b) Interference contrast micrograph at -150°C after completion of $\beta \to \gamma$ transformation.

Fig. 9: Interference contrast micrograph of a β-phase area which had undergone twice the $\beta \to \alpha$ transformation. Note superposition of 2 different domain patterns.

Fig. 10: Schematic drawing of the heating stage with which MeH samples may be heated up in air to approximately 200°C. The heater block may be tilted using the 3 screws.

Fig. 11: Polarized light sequence of the order disorder transformation $\beta \to \beta + \alpha' \to \alpha'$ in the NbH-system.

a) $T = 25^\circ$C. The whole specimen is in the ordered β-phase.

b) $T = 112^\circ$C. Some of the β-phase has locally transformed to the cubic α'-phase which appears in uniform grey.

c) $T = 113^\circ$C. Some regions of the β-phase still remain inside the α'-phase. The bulk has transformed to the cubic α'-phase.

Fig. 12: Schematic drawing of the cooling stage. Sample may be cooled to -196°C by filling the dewar with liquid nitrogen. The temperature is adjustable through the use of the heater.

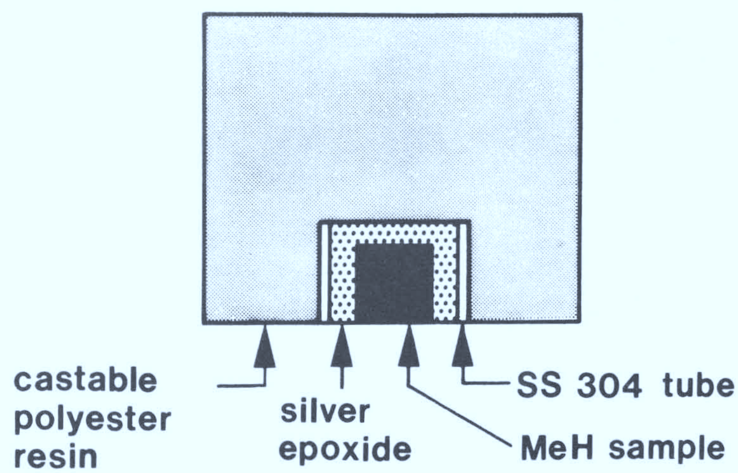
castable
polyester
resin
silver
epoxide
SS 304 tube
MeH sample

Fig. 1 (II)

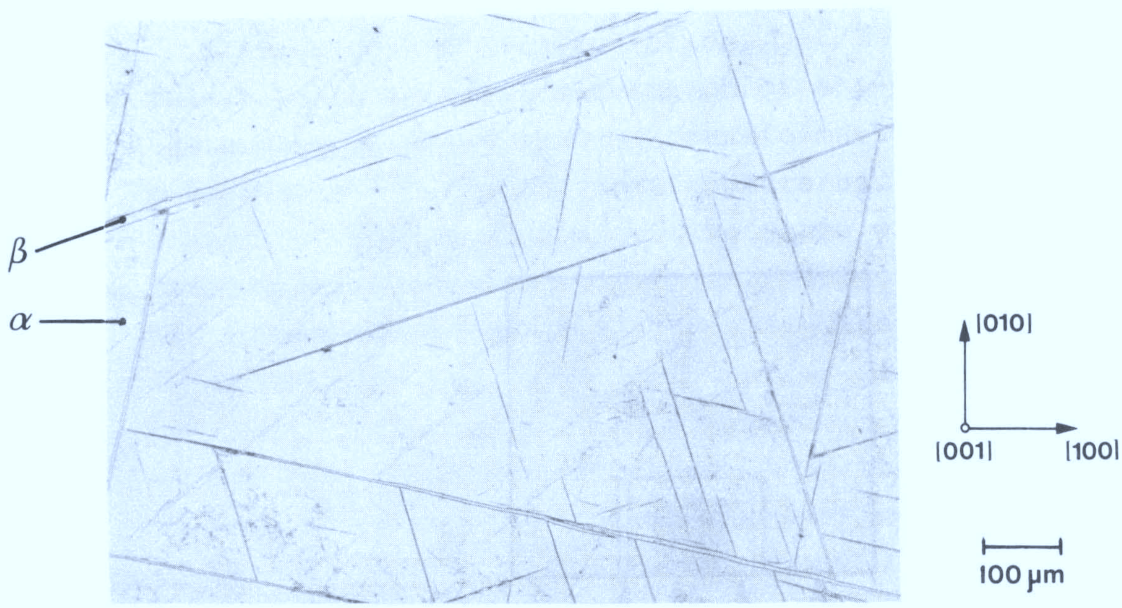

Fig. 2 (II)

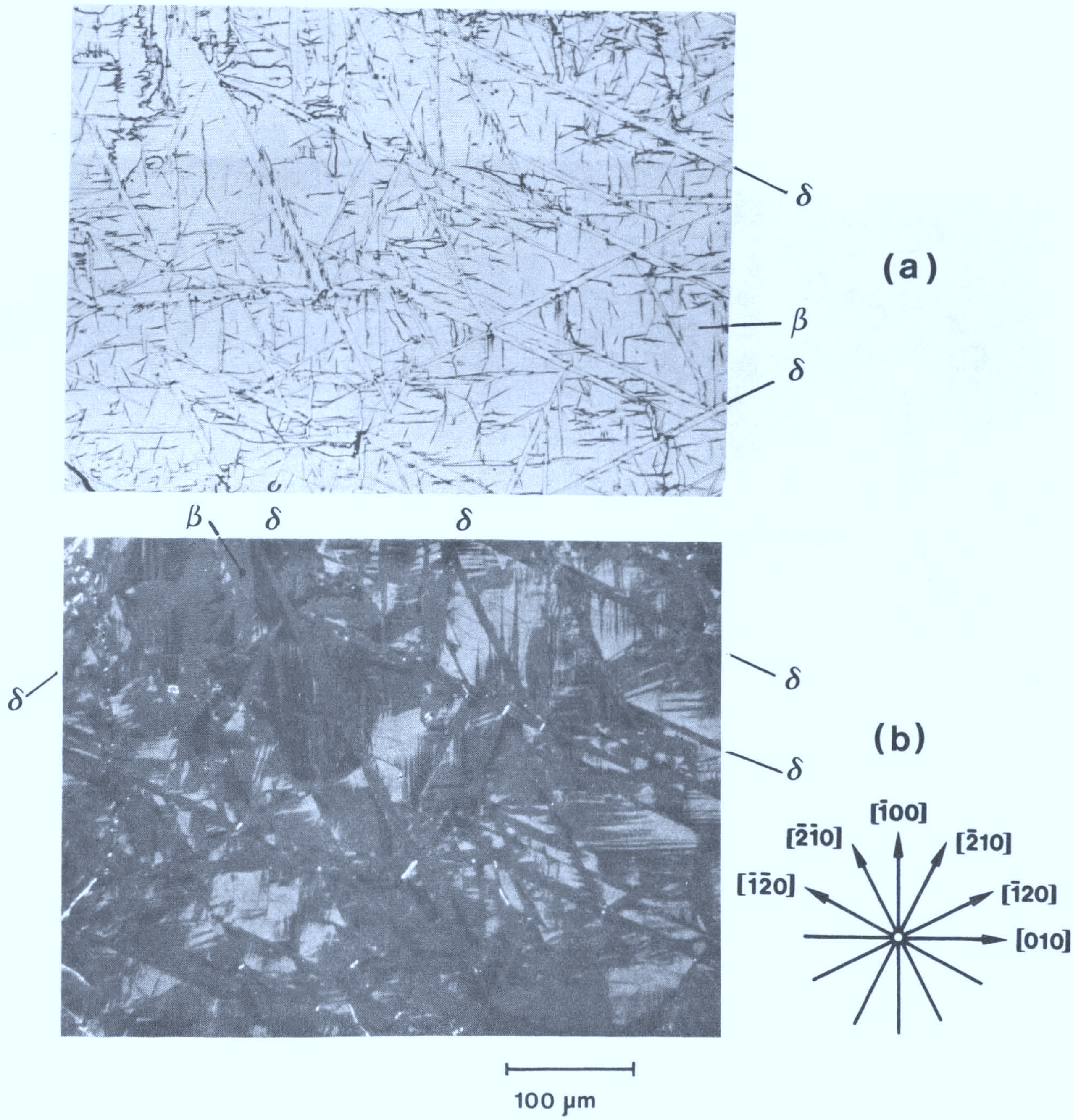

Fig. 3a,b(II)

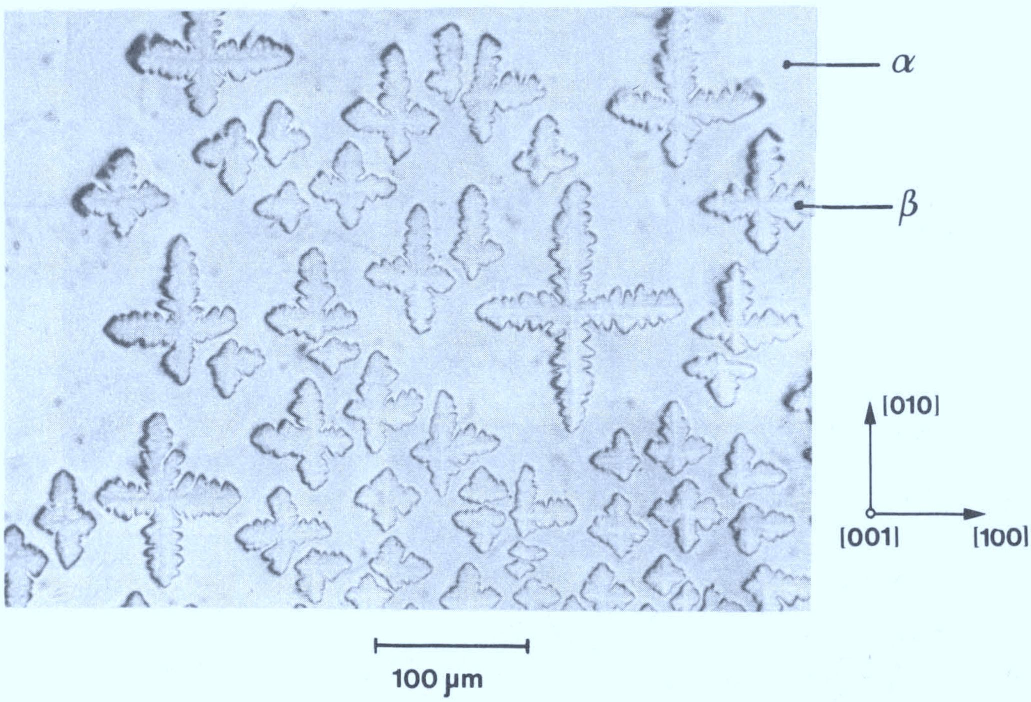

Fig. 4 (II)

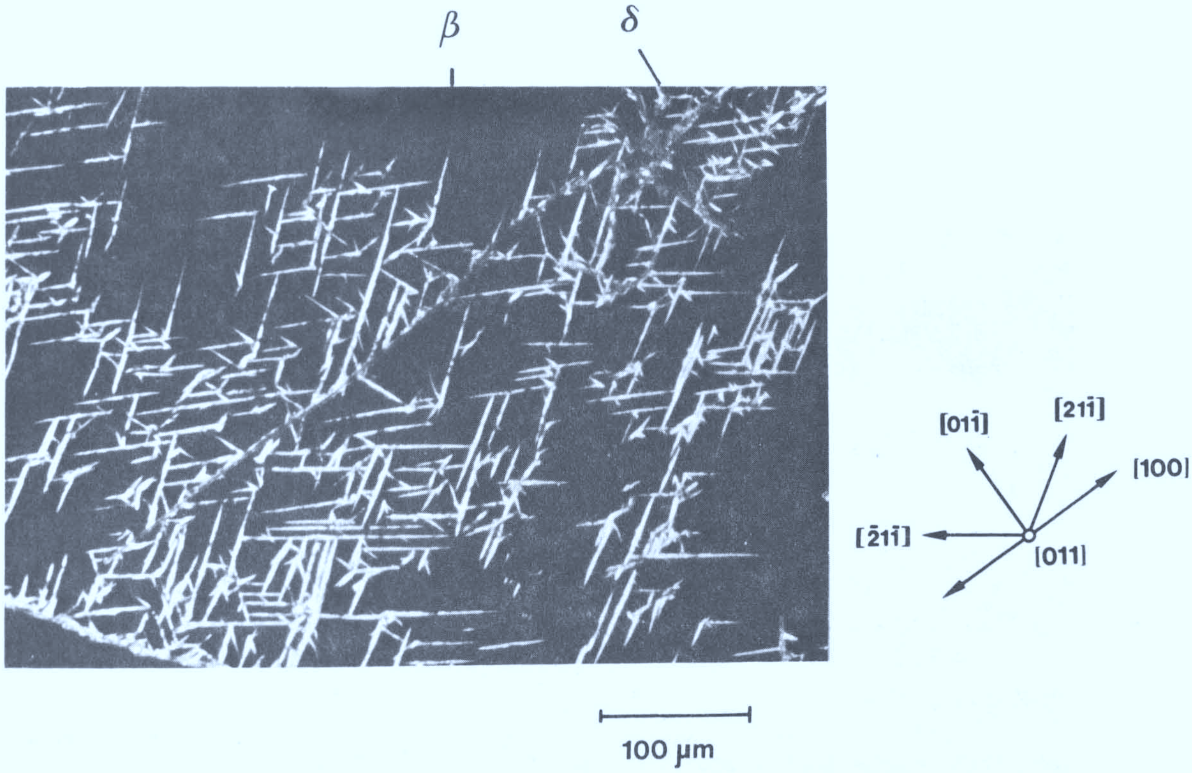

Fig. 5 (II)

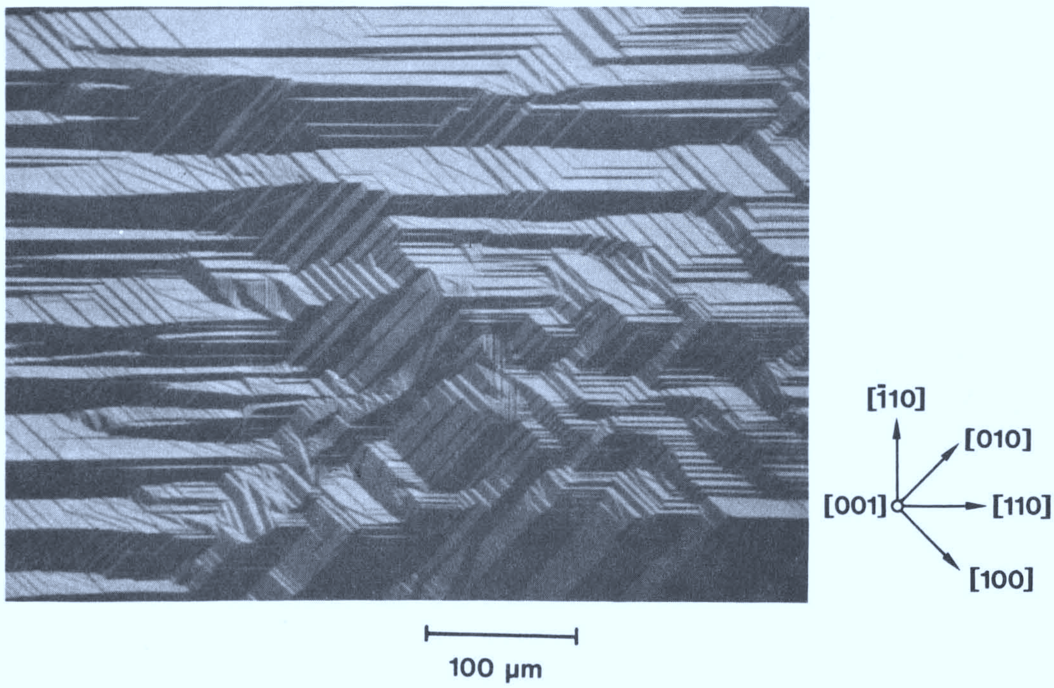

Fig. 6 (II)

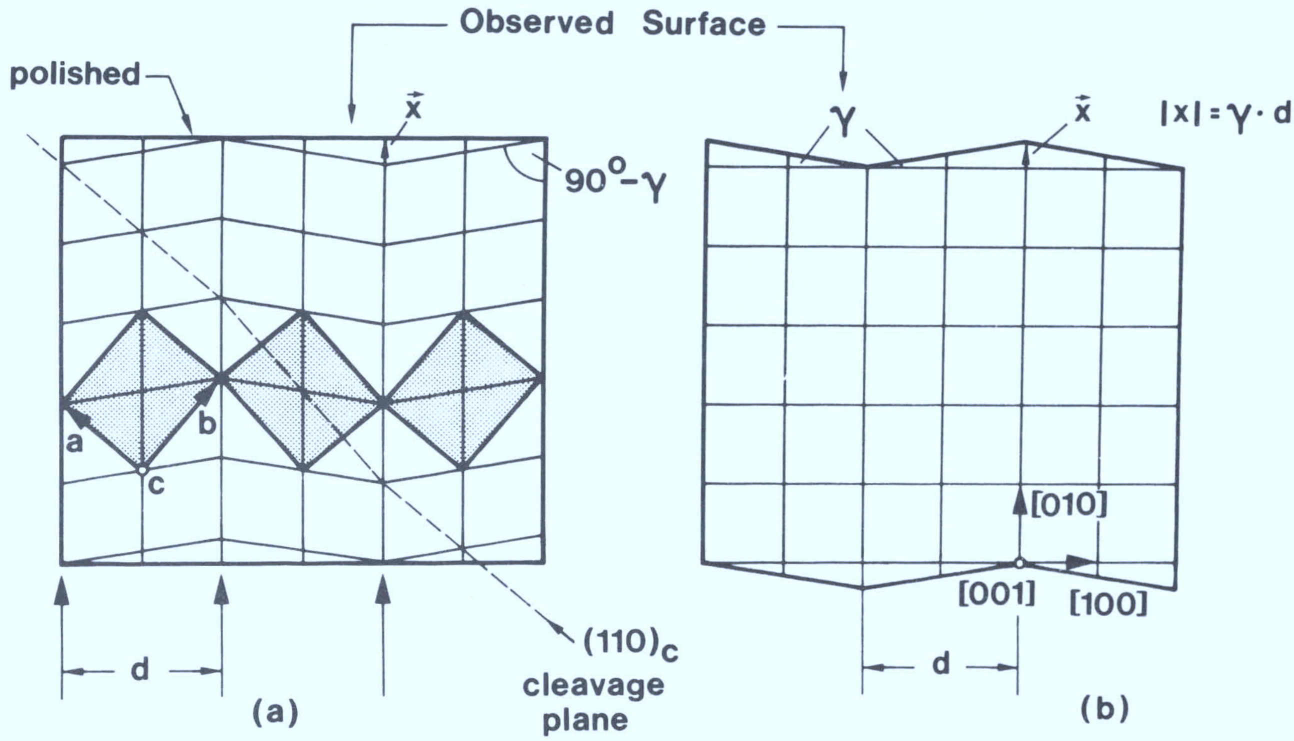

Observed Surface
polished
x
90°-γ
γ
x
|x| = γ · d
a
b
c
[010]
[001]
[100]
d
(110)c
cleavage
plane
d
(a)
(b)

Fig. 7 a,b(II)

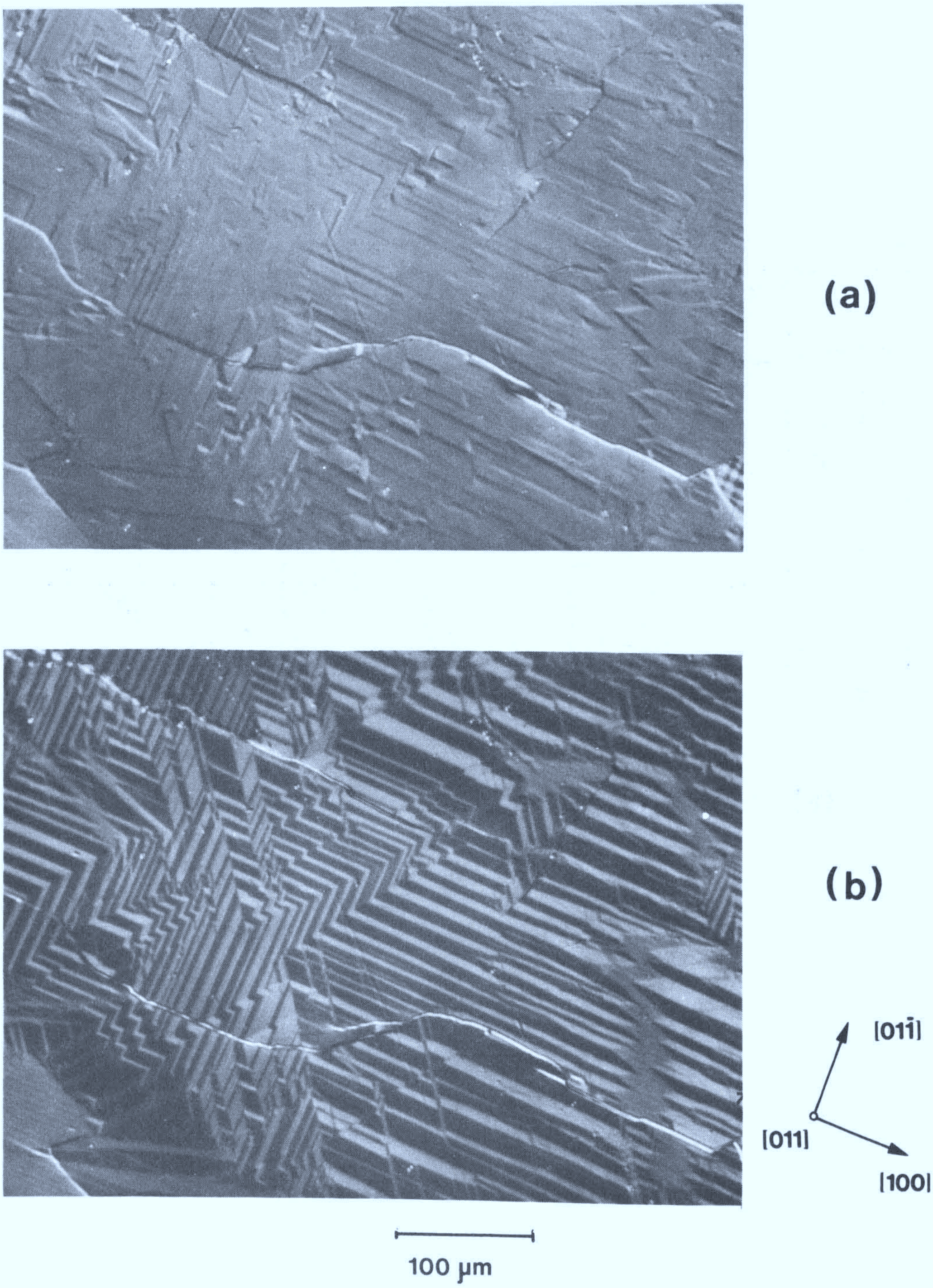

Fig. 8 a,b(II)

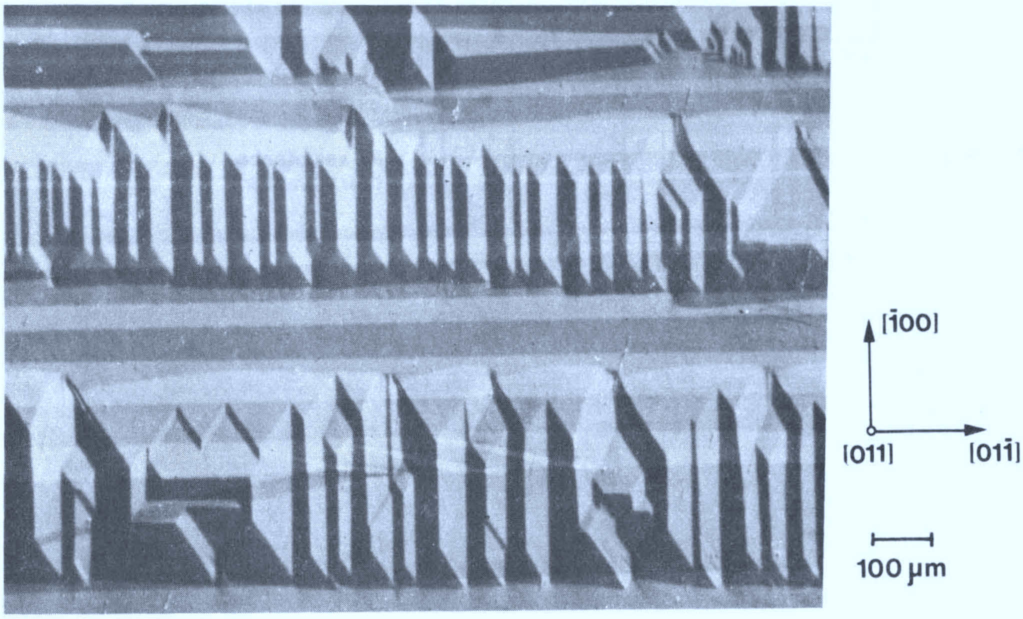

Fig. 9(II)

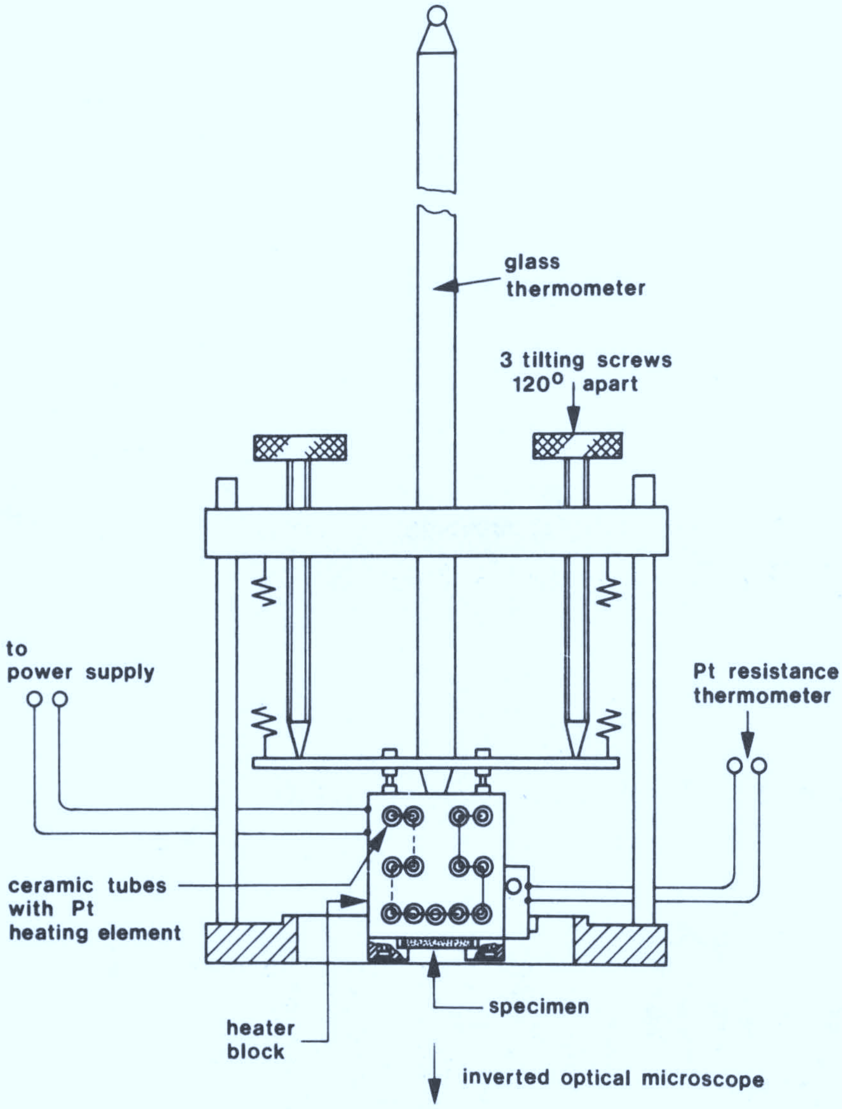
glass
thermometer
3 tilting screws
120° apart
to
power supply
Pt resistance
thermometer
ceramic tubes
with Pt
heating element
specimen
heater
block
inverted optical microscope

Fig. 10 (II)

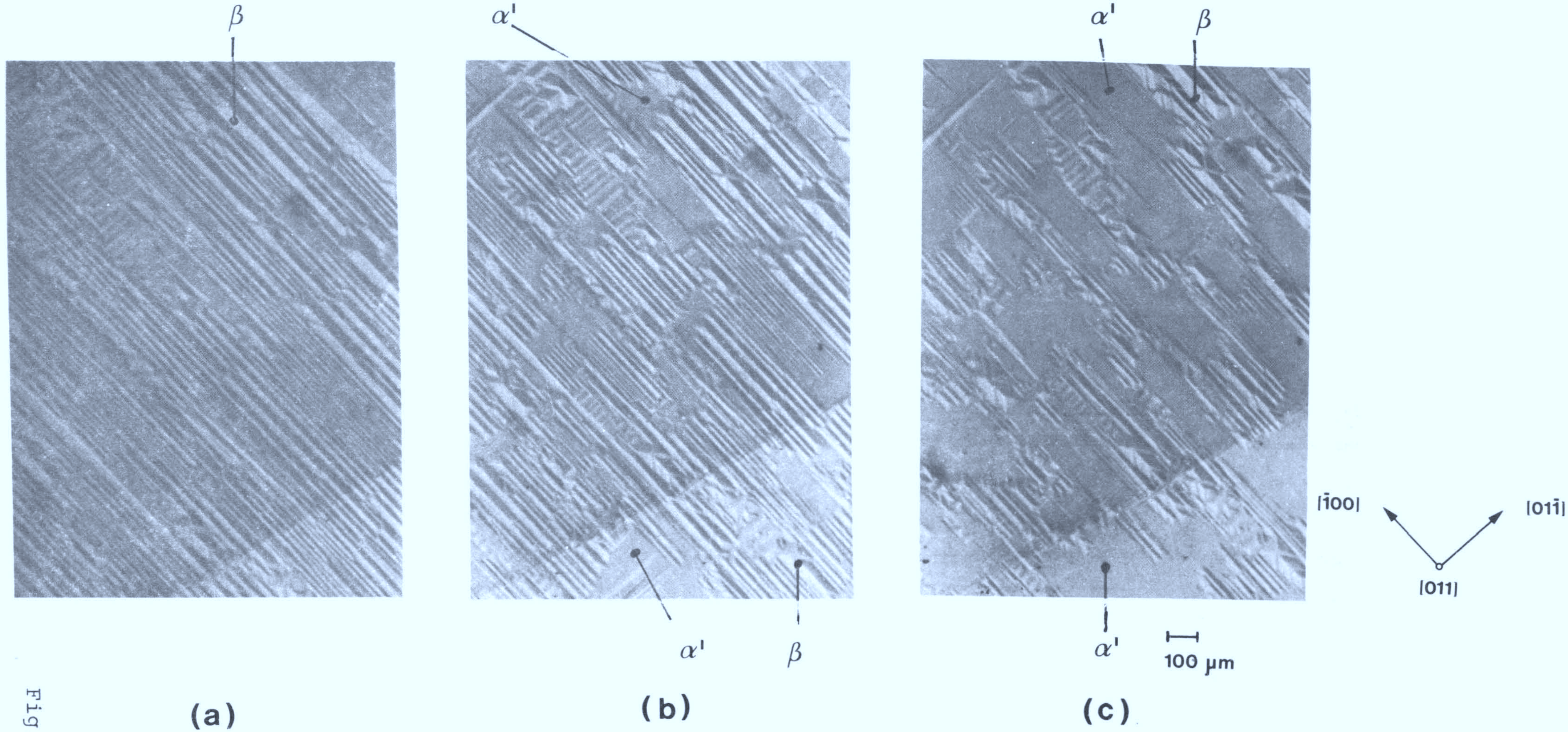

Fig. 11 a,b,c

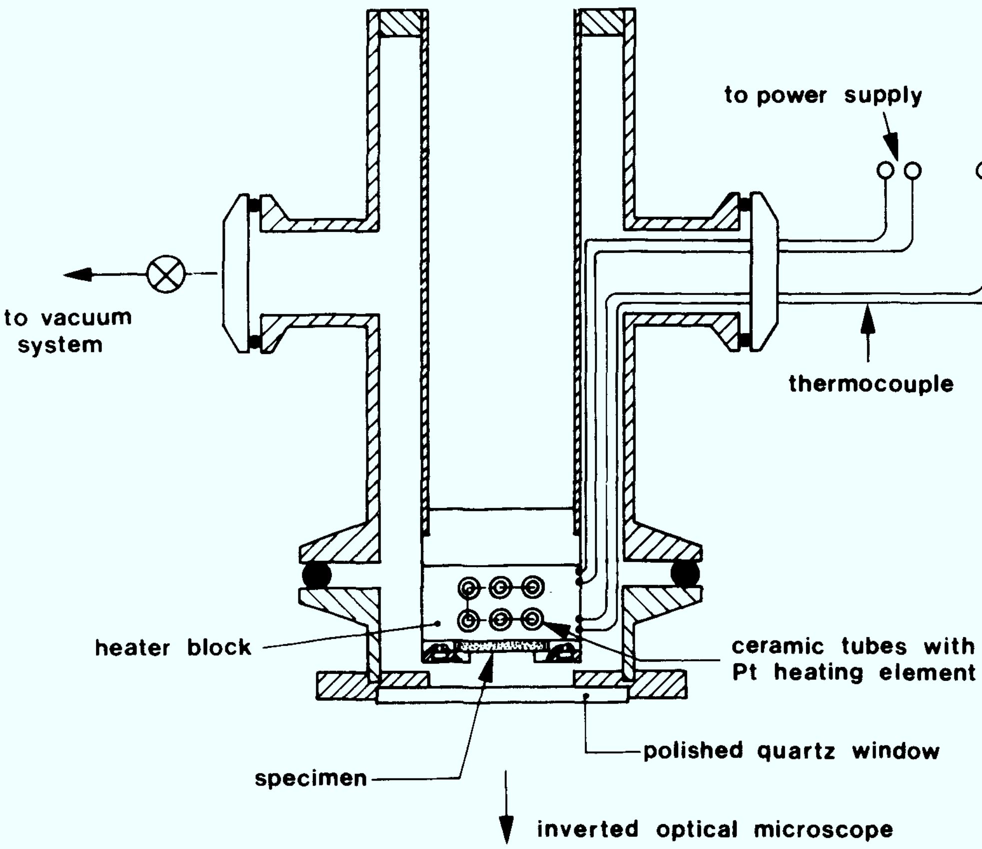
to power supply
to vacuum
system
thermocouple
heater block
ceramic tubes with
Pt heating element
polished quartz window
specimen
inverted optical microscope

Fig. 12 (II)